A Unified Micromechanical Model for the Mechanical Properties of Two Constituent Composite Materials Part II: Plastic Behavior

ZHENG-MING HUANG*
Department of Mechanics
Huazhong University of Science & Technology
Wuhan, Hubei 430074
People's Republic of China

ABSTRACT: This series of papers reports a new, general, and unified micromechanical model for estimating the three-dimensional mechanical properties of a composite made from two isotropic constituent materials, i.e., continuous fiber and matrix. The present paper concentrates on the plastic behavior of the composite. Based on a perfect bonding assumption for the fiber and matrix interface during the entire elastic-plastic deformation range under consideration, a bridging relationship connecting the internal stresses generated in the matrix with those in the fiber is dependent only on the constituent geometric and material properties. Thus, the bridging matrix used in Reference [1] for elastic deformation analysis is modified according to the changed material properties of the constituents to account for their plastic deformation effect. With this matrix, the internal stress increments in each constituent material at every load level are explicitly related to the overall stress increments on the composite. The overall instantaneous compliance matrix of the composite follows easily once the constituent compliance matrices have been defined using any existing plastic flow theory of isotropic materials. Such an instantaneous compliance matrix will be of crucial importance in failure analysis of laminated composites. Incorporation of the Prandtl-Reuss flow relations with the explicit formulae proposed for the bridging matrix in Reference [1] has been described in the present paper. Good correlation has been found between predicted and available experimental elastic-plastic stress-strain curves of several unidirectional fibrous composites subjected to both uniaxial and combined load conditions.

KEY WORDS: fiber-reinforced composite, unidirectional composite, mechanical property, elastic behavior, plastic behavior, constitutive equations, plastic flow theory, micromechanics approach, unified model.

*Present address: Department of Mechanical & Production Engineering, National University of Singapore, 10 Kent Ridge Crescent, Singapore 119260.

0892-7057/00/05 0344–19 $10.00/0 DOI: 10.1106/74AD-GXYK-6NQH-L2AV

INTRODUCTION

THE MAJORITY OF matrix materials used in fabricating composites possess the ability to undergo significant nonlinear plastic/inelastic deformation before failure. This is especially true in the case of metal- and polymer-matrix composites. In order to make full use of all the advantages of a composite material, it is necessary to understand an elastic-plastic behavior of the composite during the whole deformation range.

There are two general approaches to model the elastic-plastic behavior of the composite: macromechanical and micromechanical. In a macromechanical approach, the heterogeneous nature of the composite is replaced by a homogeneous medium with anisotropic elastic-plastic properties. Hahn and Tsai [2] proposed an elastic-plastic constitutive model by assuming different behaviors in the various lamina directions and only the nonlinearity due to in-plane shearing has been involved. Jones and Morgan [3] introduced a strain energy function that incorporated the anisotropic elastic-plastic behavior of the composite. Sun and Chen [4] treated the composite as a homogeneous orthopic elastic-plastic continuum. They used a one-parameter plastic potential function to describe the plastic strain increments of the composite.

Several different micromechanical approaches have been developed to predict the elastic-plastic response of the composite. Perhaps the simplest one is the rule-of-mixtures approximation [5]. The other earlier approaches include the self-consistent schemes [6–8], the finite element analyses [9–11], and the concentric cylinder model [12,13]. Dvorak and Bahei-El-Din [14,15] developed a vanishing fiber diameter model. This method assumes that the fibers possess a vanishingly small diameter even though they occupy a finite volume fraction of the composite. Therefore, only the longitudinal constraints between the fibers and the matrix have been considered in this model. Hopkins and Chamis [16,17] proposed a multicell model based on the response of a single representative volume element. The nonlinear thermovisco-plastic behaviour is approximated through the use of power law relations where the ratio of the property of interest to a given reference volume is set equal to a product of terms with unknown exponents. Aboudi [18] developed a continuum model that seems more promising [19–21] but is much more complicated than most of the previous approaches. In Aboudi's approach, the representative volume is further divided into subcells. Continuity and equilibrium conditions are satisfied on an average basis between subcells and neighboring cells. First order theory is incorporated in the approaches; i.e., the displacement variation in each subcell is assumed to be linear, and the stress and strain are constant in the cell. However, this relaxation of complete continuity and equilibrium requirements could lead to overlaps or gaps occurring between subcells at isolated points [20].

It can be seen from reviewing [22] these approaches that the developments in

micromechanical models for the nonlinear plastic behavior of the composite are far behind their counterparts for the linear elastic behavior of the composite. Most existing models have made some significant assumptions for the constituent plastic deformations and yet much more complicated evaluations are involved. In this paper, a general yet simple and user-friendly micromechanics modeling approach is proposed to analyze the three-dimensional elastic-plastic response of fibrous composites in which the constituent plastic behaviors can be described using any plastic flow theory. The most commonly used Prandtl-Reuss flow rule is employed in the present paper. A key step in the present approach is to use the same form of the bridging matrix as utilized in Reference [1] to correlate the stress vectors in the different phases of the composite. The unified model developed in Reference [1] is then extended to include the effect of the constituent plastic deformation. Only the material parameters involved in the independent elements of the bridging matrix need to be changed accordingly when any constituent material undergoes plastic deformation. Determination of the remaining bridging elements is the same as that described in Reference [1] for an elastic analysis. Using the bridging matrix, the incremental stresses in both the fiber and matrix materials at every load level are explicitly related to the overall stress increments applied on the composite, and the overall instantaneous compliance matrix of the composite follows easily. The proposed model has been applied to several unidirectional composites subjected to both uniaxial and combined load conditions. The predicted elastic-plastic stress-strain curves are compared with available experimental data. Good correlation has been found.

CONSTITUTIVE EQUATIONS OF ISOTROPIC MATERIALS

As the present unified model is developed based on the fact that the constitutive equations for both the constituent fiber and matrix materials are well established, application of the general Prandtl-Reuss flow theory [23] to the constituents is first summarized in this section.

Let us consider an isotropic material, either the fiber or the matrix, which may undergo elastic-plastic deformation. An incremental stress-strain relationship of the material can be expressed as

$$\{d\varepsilon_i\} = [S_{ij}]\{d\sigma_j\} \tag{1}$$

When the deformation is in a linearly elastic region, the compliance matrix $[S_{ij}]$ takes the form

$$[S_{ij}] = [S_{ij}]^e = \begin{bmatrix} [S_{ij}]_\sigma & 0 \\ 0 & [S_{ij}]_\tau \end{bmatrix} \tag{2}$$

where $[S_{ij}]_\sigma$ and $[S_{ij}]_\tau$ are the sub-matrices correlating normal stresses with elongation strains and shear stresses with shear strains, respectively, and are given by

$$[S_{ij}]_\sigma = \begin{bmatrix} \frac{1}{E} & -\frac{\nu}{E} & -\frac{\nu}{E} \\ & \frac{1}{E} & -\frac{\nu}{E} \\ \textit{symmetry} & & \frac{1}{E} \end{bmatrix} \tag{3.1}$$

$$[S_{ij}]_\tau = \begin{bmatrix} \frac{1}{G} & 0 & 0 \\ & \frac{1}{G} & 0 \\ \textit{symmetry} & & \frac{1}{G} \end{bmatrix} \tag{3.2}$$

in which E, ν, and G are the Young's modulus, Poisson's ratio, and shear modulus with

$$G = E/2(1+\nu) \tag{3.3}$$

When the deformation is in a plastic region, let us assume that the Prandtl-Reuss flow rule be applied to specify the constitutive equations of the material. Using an incremental form, this flow rule postulates that the plastic incremental strains are proportional to the total deviatoric stresses, i.e.,

$$d\varepsilon_{ij}^{(p)} = d\lambda\sigma'_{ij} \tag{4}$$

where $d\varepsilon_{ij}^{(p)}$ denote the strain increments in the plastic region, $d\lambda$ is a positive parameter, and

$$\sigma'_{ij} = \sigma_{ij} - \frac{1}{3}\sigma_{kk}\delta_{ij} \tag{5}$$

In Equation (5) and in the following, a summation convention is used for the repeated indices from 1 to 3. The parameter $d\lambda$ can be defined simply by multiplying (4) by itself. This gives

$$d\lambda = [d\varepsilon_{ij}^{(p)} d\varepsilon_{ij}^{(p)}]^{1/2} / (\sigma'_{ij}\sigma'_{ij})^{1/2} \tag{6}$$

The total strain increments can be separated into

$$d\varepsilon_{ij} = d\varepsilon_{ij}^{(e)} + d\varepsilon_{ij}^{(p)} \tag{7}$$

where the elastic components are related to the stress increments through

$$d\varepsilon_{ij}^{(e)} = \frac{1-2\nu}{3E} d\sigma_{kk}\delta_{ij} + \frac{1+\nu}{E} d\sigma_{ij} \tag{8}$$

Defining the octahedral plastic shear strain increment as

$$d\varepsilon_0^{(p)} = \left[\frac{1}{3} d\varepsilon_{ij}^{(p)} d\varepsilon_{ij}^{(p)}\right]^{1/2} \tag{9}$$

and the octahedral shear stress as

$$\tau_0 = \left[\frac{1}{3}\sigma'_{ij}\sigma'_{ij}\right]^{1/2} \tag{10}$$

Equation (6) becomes

$$d\lambda = d\,\varepsilon_0^{(p)}/\tau_0 \tag{11}$$

Substituting the last equation into Equation (4), we have

$$d\varepsilon_{ij}^{(p)} = \left(\frac{d\varepsilon_0^{(p)}}{\tau_0}\right)\sigma'_{ij} \tag{12}$$

To establish a relationship between $d\varepsilon_0^{(p)}$ and τ_0, let us apply Equation (12) to a uniaxial tensile test in which

$$\sigma_{22} = \sigma_{33} = \sigma_{12} = \sigma_{13} = \sigma_{23} = 0, \text{ and } \sigma_{11} \neq 0 \tag{13}$$

and

$$d\varepsilon_{12}^{(p)} = d\varepsilon_{23}^{(p)} = d\varepsilon_{13}^{(p)} = 0,$$

$$d\varepsilon_{22}^{(p)} = d\varepsilon_{33}^{(p)} = -\frac{1}{2} d\varepsilon_{11}^{(p)}, d\varepsilon_{11}^{(p)} \neq 0 \tag{14}$$

where the condition of plastic incompressibility has been utilized. Substituting (14) into (9) yields

$$d\varepsilon_{11}^{(p)} = \sqrt{2} d\varepsilon_0^{(p)} \tag{15}$$

while substituting (13) into (5) and then into (10) gives

$$\tau_0 = \frac{\sqrt{2}}{3}\sigma_{11} \tag{16}$$

Suppose that the tensile stress-strain curve of the material is composed of piecewise linear segments. A typical bilinear curve is shown in Figure 1. We use E_T to represent the hardening modulus (tangent to the stress-strain curve in the plastic region) of the material. Due to the well-known property in the material unloading process, the relationship between the octahedral plastic shear strain increment and the tensile stress increment can be denoted by (see Figure 1)

$$d\varepsilon_0^{(p)} = \frac{1}{\sqrt{2}}\left(\frac{1}{E_T} - \frac{1}{E}\right)d\sigma$$

since $E_T = d\sigma / d\varepsilon = d\sigma / d\varepsilon_{11}$ in the plastic region. We thus get

$$d\tau_0 = \frac{2M_T}{3} d\varepsilon_0^{(p)} \tag{17}$$

where

$$M_T = \frac{EE_T}{E - E_T} \tag{18}$$

On the other hand, differentiating (10) gives

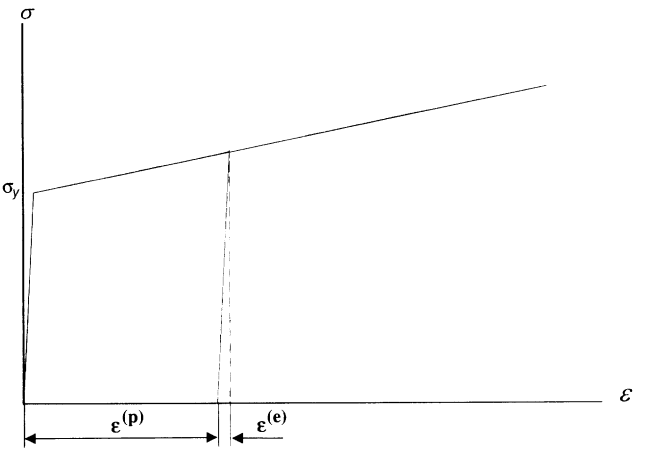

Figure 1. *A bilinear elastic-plastic stress-strain curve.*

$$d\tau_0 = \frac{\sigma'_{ij}}{3\tau_0} d\sigma'_{ij}$$

Substituting (17) into the last equation yields

$$d\varepsilon_0^{(p)} = \frac{\sigma'_{ij}}{2M_T\tau_0} d\sigma'_{ij} \tag{19}$$

From Equations (19) and (12), we obtain

$$d\varepsilon_{ij}^{(p)} = \frac{\sigma'_{kl} d\sigma'_{kl}}{2M_T\tau_0^2} \sigma'_{ij} \tag{20}$$

If we make use of the assumption that no plastic work can be done by the hydrostatic component of applied stress field, i.e.,

$$\sigma'_{ij} d\sigma'_{ij} = \sigma'_{ij}\left(d\sigma_{ij} - \frac{1}{3} d\sigma_{kk}\delta_{ij}\right) = \sigma'_{ij} d\sigma_{ij}$$

then Equation (20) is rewritten as

$$d\varepsilon_{ij}^{(p)} = \frac{\sigma'_{kl}\sigma'_{ij}}{2M_T\tau_0^2} d\sigma_{kl} \tag{21}$$

Substituting (8) and (21) into (7), we finally obtain

$$d\varepsilon_{ij} = \frac{1-2\nu}{3E} d\sigma_{kk}\delta_{ij} + \frac{1+\nu}{E} d\sigma_{ij} + \frac{\sigma'_{kl}\sigma'_{ij}}{2M_T\tau_0^2} d\sigma_{kl} \tag{22}$$

Equation (22) is the general constitutive relation governing isotropic elastic-plastic material behavior. It relates strain increments with stress increments in terms of the octahedral shear stress τ_0, which is defined by (10). Rewriting (22) in the vector form, the incremental elastic-plastic constitutive equations of an isotropic material can always be formally denoted by Equation (1), in which the compliance matrix has the form

$$[S_{ij}] = \begin{cases} [S_{ij}]^e, \text{ when } \tau_0 \le \dfrac{\sqrt{2}}{3}\sigma_Y \\ [S_{ij}]^e + [S_{ij}]^p, \text{ when } \tau_0 > \dfrac{\sqrt{2}}{3}\sigma_Y \end{cases} \tag{23}$$

where σ_Y is the uniaxial yield strength of the material, $[S_{ij}]^e$ is the elastic component of the compliance matrix given by Equations (2) and (3), and $[S_{ij}]^p$ is the plastic component defined as

$$[S_{ij}]^p = \frac{1}{2M_T\tau_0^2}\begin{bmatrix} \sigma'_{11}\sigma'_{11} & \sigma'_{22}\sigma'_{11} & \sigma'_{33}\sigma'_{11} & 2\sigma'_{23}\sigma'_{11} & 2\sigma'_{13}\sigma'_{11} & 2\sigma'_{12}\sigma'_{11} \\ & \sigma'_{22}\sigma'_{22} & \sigma'_{33}\sigma'_{22} & 2\sigma'_{23}\sigma'_{22} & 2\sigma'_{13}\sigma'_{22} & 2\sigma'_{12}\sigma'_{22} \\ & & \sigma'_{33}\sigma'_{33} & 2\sigma'_{23}\sigma'_{33} & 2\sigma'_{13}\sigma'_{33} & 2\sigma'_{12}\sigma'_{33} \\ & & & 4\sigma'_{23}\sigma'_{23} & 4\sigma'_{13}\sigma'_{23} & 4\sigma'_{12}\sigma'_{23} \\ & & & & 4\sigma'_{13}\sigma'_{13} & 4\sigma'_{12}\sigma'_{13} \\ \textit{symmetry} & & & & & 4\sigma'_{12}\sigma'_{12} \end{bmatrix} \tag{24}$$

It should be pointed out that the plastic component, $[S_{ij}]^p$, can occur only in an elastic-plastic loading situation. Whenever there is an unloading, the compliance matrix of the material is simply given by its elastic component.

ELASTIC-PLASTIC CONSTITUTIVE EQUATIONS OF THE COMPOSITE

To derive an elastic-plastic compliance matrix for the composite, let us accept the following assumptions: (a) Both the fiber and the matrix are isotropic elastic-plastic materials whose constitutive equations have the form of Equations (1) and (23); (b) the geometrical deformation of the composite is so small that the volume fractions of the fiber and the matrix, V_f and V_m, in a representative volume element (RVE) of the composite remain unchanged during an entire load sequence; and (c) each load increment is so small that whenever there is a plastic deformation, the plastic compliance component $[S_{ij}]^p$,defined by (24), will be evaluated at the beginning of the load increment under consideration and will remain constant during that load increment.

Let $\{d\sigma_i^f\}$ and $\{d\varepsilon_i^f\}$, and $\{d\sigma_i^m\}$ and $\{d\varepsilon_i^m\}$, respectively, represent the internal stress and strain increments in the fiber and matrix phases of the RVE. $\{d\sigma_i\}$ and $\{d\varepsilon_i\}$ denote the overall incremental stresses and strains of the composite in the RVE. Further, $[S_{ij}^f]$, $[S_{ij}^m]$, and $[S_{ij}]$ denote the elasto-plastic compliance matrices of the fiber, the matrix, and the composite in the RVE, respectively. At each load level, according to the assumptions (a) and (b), we have the following relationships:

$$\{d\varepsilon_i^f\} = [S_{ij}^f]\{d\sigma_j^f\} \tag{25.1}$$

$$\{d\varepsilon_i^m\} = [S_{ij}^m]\{d\sigma_j^m\} \tag{25.2}$$

$$\{d\varepsilon_i\} = V_f\{d\varepsilon_i^f\} + V_m\{d\varepsilon_i^m\} \tag{26.1}$$

$$\{d\sigma_i\} = V_f\{d\sigma_i^f\} + V_m\{d\sigma_i^m\} \tag{26.2}$$

Similar to a linear elastic analysis [1], let us assume that there is a bridging matrix such that

$$\{d\sigma_i^m\} = [A_{ij}]\{d\sigma_j^f\} \tag{27}$$

By using the assumption (c), we obtain

$$\{d\sigma_i^f\} = (V_f[I] + V_m[A_{ij}])^{-1}\{d\sigma_j\} \tag{28.1}$$

$$\{d\sigma_i^m\} = [A_{ij}](V_f[I] + V_m[A_{ij}])^{-1}\{d\sigma_j\} \tag{28.2}$$

and

$$[S_{ij}] = (V_f[S_{ij}^f] + V_m[S_{ij}^m][A_{ij}])(V_f[I] + V_m[A_{ij}])^{-1} \tag{29}$$

Equations (28.1) and (28.2) explicitly relate the internal stresses in the fiber and the matrix phases with the overall stresses applied on the composite, while Equation (29) defines the elastic-plastic compliance matrix of the composite upon the instantaneous compliance matrices of the constituent materials. The remaining question is how to define the bridging matrix, $[A_{ij}]$.

It is reasonable to assume that the bridging matrix, $[A_{ij}]$, has the same structure as that used in the linear elastic analysis (see Reference [1] for more detail), i.e., containing 5 independent elements and 16 other dependent elements [1]. Determination of the dependent elements is standard. The equations to define the independent elements should be the same. Only the appropriate Young's modulus and Poisson's ratio of a constituent material involved should be replaced by its plastic counterparts when the material undergoes a plastic deformation. This is due to the fact that the volume fractions of the fiber and the matrix do not change when the composite material undergoes deformation from the linearly elastic region to the plastic one. The fiber packing geometry, such as fiber arrangement in the matrix, fiber cross-sectional shape, etc., also remains unchanged or varies by only a negligibly small amount. More precisely, let us define effective Young's moduli and effective Poisson's ratios for the fiber and matrix materials as follows:

$$E_f = \begin{cases} E^f, \text{ when } \tau_0^f \le \dfrac{\sqrt{2}}{3}\sigma_Y^f \\ E_T^f, \text{ when } \tau_0^f > \dfrac{\sqrt{2}}{3}\sigma_Y^f \end{cases} \tag{30.1}$$

$$\nu_f = \begin{cases} \nu^f, \text{ when } \tau_0^f \le \dfrac{\sqrt{2}}{3}\sigma_Y^f \\ 0.5, \text{ when } \tau_0^f > \dfrac{\sqrt{2}}{3}\sigma_Y^f \end{cases} \tag{30.2}$$

$$E_m = \begin{cases} E^m, \text{ when } \tau_0^m \le \dfrac{\sqrt{2}}{3}\sigma_Y^m \\ E_T^m, \text{ when } \tau_0^m > \dfrac{\sqrt{2}}{3}\sigma_Y^m \end{cases} \tag{31.1}$$

$$\nu_m = \begin{cases} \nu^m, \text{ when } \tau_0^m \le \dfrac{\sqrt{2}}{3}\sigma_Y^m \\ 0.5, \text{ when } \tau_0^m > \dfrac{\sqrt{2}}{3}\sigma_Y^m \end{cases} \tag{31.2}$$

where E^f, ν^f and E^m, ν^m are, respectively, the Young's moduli and the Poisson's ratios of the fiber and the matrix materials in their linearly elastic region, E_T^f and E_T^m are the hardening moduli of the fiber and the matrix in their plastic region, τ_0^f and τ_0^m are the octahedral shear stresses in the fiber and the matrix phases, respectively, and σ_Y^f and σ_Y^m are the uniaxial yield strengths of the fiber and the matrix. Substituting the corresponding effective Young's moduli and Poisson's ratios into the formulae defining the independent elements of the bridging matrix, $[A_{ij}]$, i.e., equations (14.1)–(14.5) in Reference [1], and then determining all the other dependent elements, we can obtain an elastic-plastic compliance matrix $[S_{ij}]$ for the composite from Equation (29). However, as in a general plastic deformation situation, the plastic component $[S_{ij}^f]^p$ or $[S_{ij}^m]^p$ or both may not have exactly the same structure as its elastic counterpart $[S_{ij}^f]^e$ or $[S_{ij}^m]^e$; therefore, it is slightly more complicated to determine the remaining dependent elements of the bridging matrix, $[A_{ij}]$. Let us explain this by using the explicit formulae for the independent elements given in Reference [1], i.e.,

$$a_{11} = E_m / E_f \tag{32.1}$$

$$a_{22} = a_{33} = 0.5(1 + E_m / E_f) \tag{32.2}$$

$$a_{55} = a_{66} = 0.5(1 + G_m / G_f) \tag{32.3}$$

where the effective shear moduli, G_m and G_f, are defined according to Equation (32.3) by means of the corresponding effective Young's modulus and Poisson's ratio. The condition that

$$(V_f S_{44}^f + V_m S_{44}^m a_{44})(V_f + V_m a_{44})^{-1} = S_{44} = 1/G_{22} = 2(1+\nu_{23})/E_{22} = 2(S_{22} - S_{23})$$

gives the element a_{44} as

$$a_{44} = \frac{V_f(G_{23} - G_f)G_m}{V_m(G_m - G_{23})G_f}, \text{ when } G_m \neq G_{23}; \text{ while } a_{44} = \frac{V_f}{V_m}, \text{ when } G_m = G_{23} \quad (32.4)$$

where

$$G_{23} = \frac{(V_f + V_m a_{11})(V_f + V_m a_{22})^2}{2(d_1 + d_2)} \quad (33.1)$$

with

$$d_1 = S_{22}^f[V_f^3 + V_m V_f^2(a_{11} + a_{22}) + V_f V_m^2 a_{11} a_{22}] + S_{22}^m[V_f V_m(V_f + V_m a_{33} + V_m a_{11})a_{22}$$

$$+ V_m^3 a_{11} a_{22} a_{33}] - V_f V_m(V_f + V_m a_{33})(S_{12}^f - S_{12}^m)a_{12}^* \quad (33.2)$$

$$d_2 = V_f V_m(V_f + V_m a_{33})(S_{12}^f - S_{12}^m)a_{12}^* - S_{12}^f[V_f^3 + V_f V_m(V_f + V_m a_{11})a_{22}]$$

$$-S_{23}^m[V_f V_m(V_f + V_m a_{22} + V_m a_{11})a_{22} + V_m(V_f^2 + V_m^2 a_{22} a_{33})a_{11}] \quad (33.3)$$

and

$$a_{12}^* = (S_{12}^f - S_{12}^m)(a_{11} - a_{22})/(S_{11}^f - S_{11}^m) \quad (33.4)$$

It should be noted that the S_{ij}^f and S_{ij}^m in Equations (33.2)–(33.4) are not necessarily the same as those in Equations (25.1) and (25.2). They are defined by Equations (2) and (3) with the corresponding effective moduli instead of the elastic ones, i.e., $S_{22}^f = S_{11}^f = 1/E_f$, $S_{23}^f = S_{12}^f = -\nu_f/E_f$, $S_{22}^m = S_{11}^m = 1/E_m$, and $S_{23}^m = S_{12}^m = -\nu_m/E_m$. The bridging matrix $[A_{ij}]$ can then be expressed as

$$[A_{ij}] = \begin{bmatrix} a_{11} & a_{12} & a_{13} & a_{14} & a_{15} & a_{16} \\ & a_{22} & a_{23} & a_{24} & a_{25} & a_{26} \\ & & a_{33} & a_{34} & a_{35} & a_{36} \\ & & & a_{44} & a_{45} & a_{46} \\ & & & & a_{55} & a_{56} \\ zero & & & & & a_{66} \end{bmatrix} \tag{34}$$

Except for the zero elements and the elements on the diagonal, which are defined by Equations (32.1)–(32.4), the other fifteen elements in (34) are all unknown as yet. They will be determined by substituting (34) into (29) and making the resulting compliance matrix satisfy symmetric conditions, i.e.,

$$S_{ji} = S_{ij} \text{ for all } i, j = 1, 2, \ldots, 6, i \neq j$$

Fifteen simultaneous algebraic equations will have to be solved to determine these elements for a most general case. However, due to the triangular feature of Equation (34), the resulting compliance matrix, Equation (29), can be explicitly expressed upon the unknown elements in (34). This will make it much easier to solve the equations. Furthermore, if there is no coupling between the normal and shear stresses for any constituent, the plastic compliance component of the material, defined by Equation (24), will have the same structure as its elastic component. In such a case, all the unknown elements in Equation (34) can be solved explicitly, as has been done in Reference [1].

SIMULATION PROCEDURE

In summation, the procedure for determination of the elastic-plastic compliance matrix of a unidirectional fiber-reinforced composite can be expressed in the following steps:

1. Input the constituent material properties, $E^f, \nu^f, E^m, \nu^m, E_T^f, E_T^m, \sigma_Y^f$ and σ_Y^m, together with volume fractions, V_f and V_m; determine the initial bridging matrices $[A_{ij}]$ and $[B_{ij}] = (V_f[I] + V_m[A_{ij}])^{-1}$ and the composite compliance matrix $[S_{ij}]$ by using a linearly elastic condition.
2. For the given overall stress increment $\{d\sigma_i\}$, evaluate the stress increments $\{d\sigma_i^f\} = [B_{ij}]\{d\sigma_j\}$ and $\{d\sigma_i^m\} = [A_{ij}]\{d\sigma_j^f\}$ in the constituent phases from Equations (28.1) and (28.2); evaluate the overall strain increment, $\{d\varepsilon_i\} = [S_{ij}]\{d\sigma_j\}$.

3. Update the total stresses and strains (initially zeros if no residual values involved):

$$\{\sigma_i\} = \{\sigma_i\} + \{d\sigma_i\}$$

$$\{\sigma_i^f\} = \{\sigma_i^f\} + (d\sigma_i^f\}$$

$$\{\sigma_i^m\} = \{\sigma_i^m\} + \{d\sigma_i^m\}$$

$$\{\varepsilon_i\} = \{\varepsilon_i\} + \{d\varepsilon_i\}$$

4. Evaluate the octahedral shear stresses τ_0^f and τ_0^m from Equation (10) by using updated $\{\sigma_i^f\}$ and $\{\sigma_i^m\}$; define new compliance matrices $[S_{ij}^f]$ and $[S_{ij}^m]$ for the constituents according to Equation (23).
5. Evaluate the effective Young's moduli and Poisson's ratios from Equations (30) and (31) and define the diagonal elements of a new bridging matrix $[A_{ij}]$ using Equations (32.1)–(32.4); solve nonlinear equations if necessary to determine the remaining elements of $[A_{ij}]$; set $[B_{ij}] = (V_f[I]+V_m[A_{ij}])^{-1}$; obtain the new overall compliance matrix $[S_{ij}]$ from Equation (29); go to Step (2) if necessary.

Steps (2) to (5) should be repeated until the overall total stresses, $\{\sigma_i\}$, reach the last level. The updated overall stresses $\{\sigma_i\}$ at each load level can be plotted against the overall strains $\{\varepsilon_i\}$ at the same level if required. These plots will give the stress-strain curves of the composite during a specified loading interval.

NUMERICAL EXAMPLES

To examine the efficiency of the micromechanics model developed above, let us apply the simulation procedure described in Section 4 to three unidirectional composites for which experimental data are all available. All the composite materials are made from boron (B) fiber and an aluminum (Al) matrix, in which the boron is considered as linearly elastic until rupture, while the aluminum is elastic-plastic. However, as the experiments were carried out independently, the constituent material properties reported were different from each other. The first example is a B-Al composite with fixed fiber volume fraction. The response of the composite subjected to off-axis loading is investigated. The loading direction has an inclined angle θ with the fiber direction. Let σ_θ represent applied stress along the loading direction. It will result in the overall stresses in the composite as

$$\sigma_1 = \sigma_{11} = \sigma_\theta \cos^2 \theta$$

$$\sigma_2 = \sigma_{22} = \sigma_\theta \sin^2 \theta$$

$$\sigma_6 = \sigma_{12} = -\sigma_\theta \sin\theta\cos\theta$$

On the other hand, the elongation strain, ε_θ, in the loading direction is calculated from the following equation:

$$\varepsilon_\theta = \varepsilon_1\cos^2\theta + \varepsilon_2 \sin^2\theta - \varepsilon_6 \sin\theta\cos\theta = \varepsilon_{11}\cos^2\theta + \varepsilon_{22}\sin^2\theta - 2\varepsilon_{12}\sin\theta\cos\theta$$

The predicted results from the present model and the experimental data taken from Reference [4] for $\theta = 10°$, 20°, 30°, and 45° are shown in Figure 2. The constituent parameters (taken from Reference [20]) used are $E^f = E_T^f = 379.3$ GPa, $\nu^f = 0.1$, $E^m = 68.3$ GPa, $E_T^m = 1.17$ GPa, $\nu^m = 0.3$, $\sigma_Y^m = 50$ MPa, $V_f = 0.475$ and $V_m = 0.525$. It can be seen from the figure that correlation between the predicted results and the experimental data is fairly good.

The second example studies the influence of the fiber volume fraction on the elastic-plastic behavior of the composite. B-Al composites with $V_f = 0.092, 0.140, 0.215$, and 0.455 under longitudinal load condition ($\theta = 0$) are considered. Predicted stress-strain results are indicated in Figure 3. Experimental data for these composites, taken from Reference [24], are also shown in the figure for comparison. All the constituent parameters used except E_T^m are taken from Reference [24].

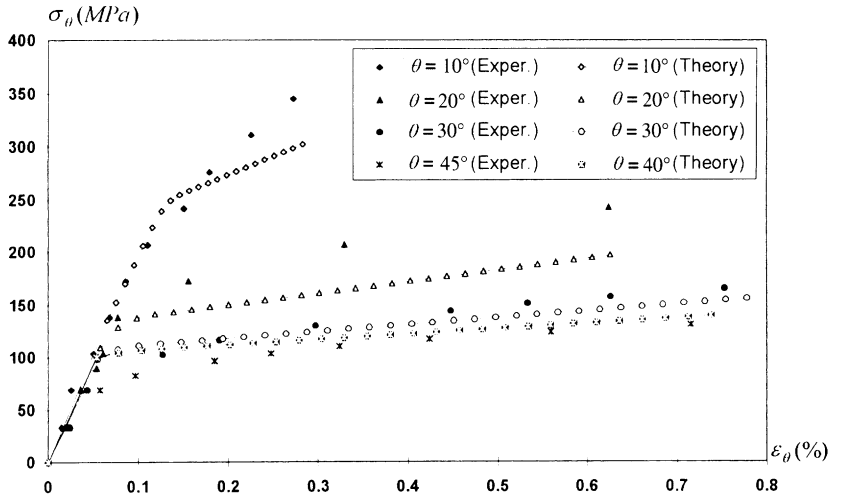

Figure 2. *Predicted and measured off-axial stress-strain response of a B-Al composite under unidirectional load.*

There was no hardening modulus for the aluminum matrix reported in Reference [24]. However, this hardening modulus cannot be zero in the Prandtl-Reuss theory employed in the present model, as can be seen from Equations (18) and (24). To resolve this problem, the datum used for E_T^m in the first example is also utilized in the present example. Thus, the material properties used are $E^f = E_T^f$ =397 GPa, $\nu^f = 0.21$, E^m = 71 GPa, E_T^m = 1.17 GPa, $\nu^m = 0.32$, and σ_y^m =142 MPa. With these parameters, the predicted stress-strain curves agree well with the measured data, as can be seen from Figure 3.

The third example is more complicated. Experimental data for the problem under consideration are taken from the results reported in Reference [25]. In the present case, the unidirectional composite, in tube form, is subjected to combined axial tension and torsion loads. The whole load sequence consists of several load paths, some of which are reversed in load direction from the others. The details can be found in Figures 11 and 12 in Reference [25]. To simulate this complicated load sequence, a number of load intervals have been chosen in which some intervals are considered as loading and the others as unloading. Whenever there is one stress component (called the *key stress component*) which begins to change its direction from the previous load condition, it is considered to begin a new loading or unloading interval. Each loading or unloading process continues until the key stress component reaches zero. Then a reversed unloading or loading process is considered to start. Each load interval is either loading or unloading. The entire load sequence is divided into 16 load intervals in which 9 are loading and 7 are unloading. They are listed in Table 1, in which endpoint values of the intervals are also given. These values are measured from Figures 11, 12, and 26 in Reference [25].

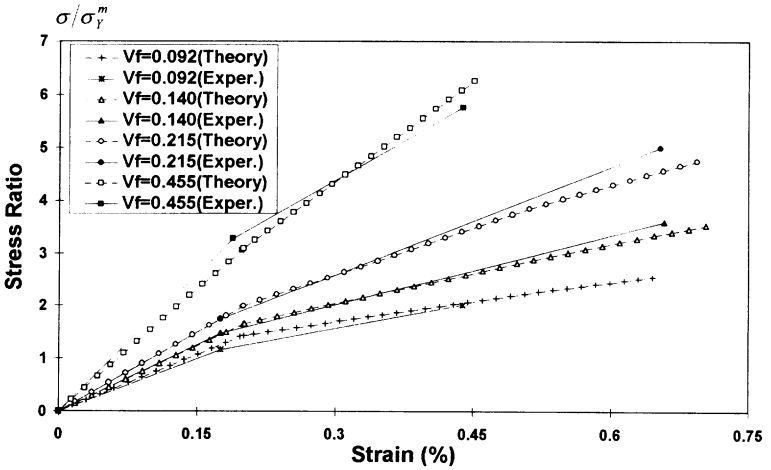

Figure 3. *Predicted and measured uniaxial stress-strain response of a B-Al composite with different fiber volume fractions (V_f).*

Table 1. Key points in the load sequence of the third example.

	Magnitude			Magnitude			Magnitude	
Point	σ_{11} (MPa)	σ_{21} (MPa)	Point	σ_{11} (MPa)	σ_{21} (MPa)	Point	σ_{11} (MPa)	σ_{21} (MPa)
O	0	0	A	0	18	B	0	54
B′	0	0	C	0	−62	D	62	−52
D′	62	0	E	62	64	E′	62	0
F	62	−63.4	F′	62	0	G	62	4
H	48	0	J	180	0	K	180	73
K′	180	0	L	180	−69			

Load sequence: O to A (loading); A to B (loading); B to B′ (unloading); B′ to C (loading); C to D (unloading); D to D′ (unloading); D′ to E (loading); E to E′ (unloading); E′ to F (loading); F to F′ (unloading); F′ to G (loading); G to H (unloading); H to J (loading); J to K (loading); K to K′ (unloading); K′ to L (loading).

It is known that the in-situ matrix properties depend on the processing procedure and may be much different from the bulk matrix properties [26]. Also, the yield strengths of a material in different load directions are usually different from each other. As relevant parameters are not available from Reference [25], three piecewise linear segments are used to approximate the tensile stress-strain curve of the aluminum plotted in Figure 27 in Reference [25] to obtain the matrix hardening moduli. The elastic constants of the boron are inversely calculated from the overall properties given in Table 1 in Reference [25]. The experimental stress-strain curve of the first two load paths, shown in Figure 26 in Reference [25], is used to adjust the matrix yield strengths corresponding to the positive shear load as well as the negative shear load. The material properties are thus chosen as: $E^f = E_T^f = 445$ GPa, $\nu^f = 0.17$, $E^m = 72.39$ GPa, $\nu^m = 0.33$, and

$$E_T^m = \begin{cases} 23.1 \text{ GPa, when } \sigma_Y^m < \sigma^m \le \sigma_Y^m + 14(\text{MPa}) \\ 6.9 \text{ GPa, when } \sigma_Y^m + 14(\text{MPa}) < \sigma^m \le \sigma_Y^m + 32(\text{MPa}) \\ 1.9 \text{ GPa, when } \sigma^m > \sigma_Y^m + 32(\text{MPa}) \end{cases}$$

where σ_Y^m is the yield strength of the matrix (aluminum) which is 40 MPa for the positive shear load and 30 MPa for the negative shear load and $\sigma^m = 3\tau_0^m/\sqrt{2}$. The fiber volume fraction, V_f, is 0.45 [25]. The predicted results using these parameters as well as the experimental data taken from Reference [25] are plotted in Figure 4. It can be seen from the figure that the predicted stress-strain curve is continuous from the load points G to J, whereas the experimental curve of this part is interrupted. Actually, the stress-strain curve for the load path from points G to J cannot be interrelated from Figure 26 in Reference [25]. Nevertheless, most parts of the

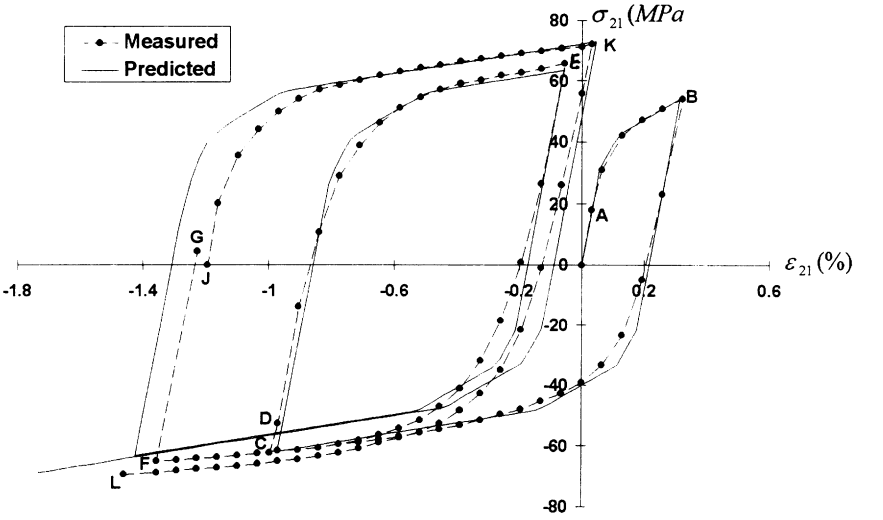

Figure 4. *Predicted and measured shear stress-shear strain response of a B-Al composite under combined tension-torsion loads.*

stress-strain curves from the prediction and the experiment agree quite well, as indicated in the figure.

CONCLUSION

The unified micromechanical model developed in Reference [1] is extended in this paper to predict the elastic-plastic behavior of a two-constituent composite material. The model uses a similar bridging matrix as employed in Reference [1] to correlate the internal stress increments generated in the two constituent phases. Only the material parameters involved in the bridging matrix need to be changed accordingly when any constituent undergoes a plastic deformation. With this bridging matrix, and as long as the elasto-plastic constitutive equations of the constituent materials are specified, the overall compliance matrix of the composite at any load level follows easily. This instantaneous compliance matrix, generally not a constant quantity, is crucial for laminate failure analysis, as will be shown in the fifth part of this series of papers. Incorporation of the Prandtl-Reuss flow relations with the explicit bridging elements proposed in Reference [1] is elaborated in the present paper. However, any other plasticity theory of isotropic materials is also applicable. Comparison between the predicted elastic-plastic stress-strain curves and the available experimental data for three unidirectional composites indicates that the present model is efficient.

REFERENCES

1. Huang, Z. M., A Unified Micromechanical Model for the Mechanical Properties of Two Constituent Composite Materials. Part I: Elastic Behaviour, *J. Thermoplastic Composite Materials* (in press).
2. Hahn, H. T. and Tsai, S. W., 1973, Nonlinear Elastic Behaviour of Unidirectional Composite Laminates, *Journal of Composite Materials,* Vol. 7, pp. 102–110.
3. Jones, R. M. and Morgan, H. S., 1977, *AIAA Journal,* Vol. 15, p. 1669.
4. Sun, C. T. and Chen, J. L., 1989, A Simple Flow Rule for Characterizing Nonlinear Behavior of Fiber Composites, *Journal of Composite Materials,* Vol. 23, pp. 1009–1020.
5. Schaffer, B. W., 1968, Elastic-Plastic Stress Distribution within Reinforced Plastics Loaded Normal to Their Internal Filaments, *AIAA Journal,* Vol. 6, pp. 2316–2324.
6. Hill, R., 1964, Theory of Mechanical Properties of Fiber-Strengthened Materials, II. Inelastic Behavior, *J. of the Mechanics & Physics of Solids,* Vol. 12, pp. 213–218.
7. Hill, R., 1965, Theory of Mechanical Properties of Fiber-Strengthened Materials, III. Self-Consistent Model, *J. of the Mechanics & Physics of Solids,* Vol. 13, pp. 189–198.
8. Huang, W., 1973, Elastoplastic Transverse Properties of a Unidirectional Fiber Reinforced Composites, *Journal of Composite Materials,* Vol. 7, pp. 482–499.
9. Adams, D. F., 1970, Inelastic Analysis of a Unidirectional Composite Subjected to Transverse Normal Loading, *Journal Composite Materials,* Vol. 4, pp. 310–328.
10. Foye, R. L., 1973, Theoretical Post-Yielding Behavior of Composite Laminates, Part I—Inelastic Micromechanics, *Journal of Composite Materials,* Vol. 7, pp. 178–193.
11. Lin, T. H., Salinas, D. and Ito, Y. M., 1972, Initial Yield Surface of a Unidirectionally Reinforced Composite, *ASME J. Appl. Mech.,* Vol. 39, pp. 321–326.
12. Jones, R. M., *Mechanics of Composite Materials,* Hemisphere Publishing Corporation, 1975, pp. 106–107.
13. Coker, D., Ashbaugh, N. E., and Nicholas, T., 1993, Analysis of the Thermomechanical Cyclic Behavior of Unidirectional Metal Matrix Composites, *Thermomechanical Fatigue Behavior of Materials, ASTM STP 1186,* Sehitoglu ed., pp. 50–69.
14. Dvorak, G. J. and Bahei-El-Din, Y. A., 1979, Elastic-Plastic Behavior of Fibrous Composites, *J. of Mechanics & Physics of Solids,* Vol. 27, pp. 51–72.
15. Dvorak, G. J. and Bahei-El-Din, Y. A., 1982, Plasticity Analysis of Fibrous Composites, *ASME J. Appl. Mech.,* Vol. 49, pp. 327–335.
16. Hopkins, D. A. and Chamis, C. C., 1985, A Unique Set of Micromechanics Equations for High Temperature Metal Matrix Composites, NASA TM 87154, Prepared for the First Symposium on Testing Technology of Metal Matrix Composites Sponsored by ASTM, Nashville, Nov. 18–20.
17. Chamis, C. C. and Hopkins, D. A., 1988, Thermoviscoplastic Nonlinear Constitutive Relationships for Structural Analysis of High Temperature Metal Matrix Composites, Testing Technology of Metal Matrix Composites, *ASTM STP 964,* P. R. DiGiovanni & N. R. Adsit eds., Philadelphia, pp. 177–196.
18. Aboudi, J., 1982, A Continuum Theory for Fiber-Reinforced Elastic-Viscoplastic Composites, *Int. J. of Eng. Sci.,* Vol. 20, pp. 605–621.
19. Aboudi, J., 1996, Micromechanical Analysis of Composites by the Method of Cells—Update, *Appl. Mech. Rev.,* Vol. 49, No. 10, pp. S83–S91.
20. Robertson, D. D. and Mall, S., 1993, Micromechanical Relations for Fiber-Reinforced Composites Using the Free Transverse Shear Approach, *J. of Composites Technology & Research,* Vol. 15, pp. 181–192.
21. Arnold, S. M., Pindera, M. J., and Wilt, T. E., 1996, Influence of Fiber Architecture on the Inelastic Response of Metal Matrix Composites, *Int. J. of Plasticity,* Vol. 12, pp. 507–545.
22. Robertson, D. D. and Mall, S., Micromechanical Analysis and Modeling, in *Titanium Matrix*

Composites-Mechanical Behavior, S. Mall & T. Nicholas eds., Technomic Publishing Co., Inc., Lancaster, 1997, pp. 397–463.

23. Adams, D. F., 1974, Elastoplastic Behavior of Composites, in *Mechanics of Composite Materials,* G. P. Sendeckyj ed., Academic Press, New York, pp. 169–208.
24. Isupov, L. P., 1996, A Variant of the Theory of Plasticity of Two-Phase Composite Media, *Acta Mechanica,* Vol. 119, pp. 65–78.
25. Dvorak, G. J., Bahei-El-Din, Macheret, Y. and Liu, C. H., 1988, An Experimental Study of Elastic-Plastic Behavior of A Fibrous Boron-Aluminum Composite, *J. of Mechanics & Physics of Solids,* Vol. 36, pp. 655–687.
26. Gates, T. S., Chen, J.-L., and Sun, C.T., Micromechanical Characterization of Nonlinear Behavior of Advanced Polymer Matrix Composites, *Composite Materials: Testing and Design (12th Vol.), ASTM STP 1274,* R. B. Deo and C. R. Saff, eds., American Society for Testing and Materials, 1996, pp. 295–319.